ABSTRACT

VALIDATION OF NEW BRAIN MRI BIOMARKERS IN PARKINSON'S DISEASE : THE USE OF QUANTITATIVE MULTI-PARAMETER MAPPING

F. Depierreux[1,2,4] , E. Parmentier[1,2,4], K.A. Baquero[1,2], E. Balteau[2], C. Phillips[3], P. Maquet[2,4], G. Garraux[1,2,4]

[1]Movere Group, [2]GIGA-CRC in vivo imaging, [3]GIGA in silico medicine, *University of Liège, Liège, Belgium,*

[4]Department of Neurology, University Hospital Center (CHU), *University of Liège, Liège, Belgium*

INTRODUCTION

The accurate diagnosis of Parkinson's disease (PD) and other related disorders (e.g. atypical Parkinson's disease) remains a challenge as it remains based on clinical features (Antoniades and Barker, 2008; Pyatigorskaya et al., 2014). In idiopathic Parkinson's disease, clinical brain magnetic resonance imaging (MRI) is usually normal, and there are no established MRI features positively supporting a diagnosis of PD(Michaeli et al., 2007). Recently, some advances have been made, both in structural and functional imaging to improve the capacity of MRI to detect changes in PD(Baudrexel et al., 2010; Pyatigorskaya et al., 2014).

We have chosen to employ a multi-echo sequence to generate quantitative multi-parameter maps (MPM) and find an appropriate MRI biomarker of PD. Quantitative MRI reveals the physical properties of the tissues, that govern MRI contrasts(Callaghan et al., 2014). The following major parameters have been investigated: longitudinal relaxation rate (R1 = 1/T1), effective transverse relaxation rate (R2*= 1/T2*), magnetization transfer saturation (MT) and effective proton density (PD*). Our hypothesis posits that these sequences show differences between PD patients and controls, revealing changes in the microstructure of brain tissues due to the pathological process seen in the disease.

MATERIAL AND METHODS

42 PD patients "on" medication and 42 healthy controls matched for age, gender and levels of education have been scanned (see details in table below).

	Healthy subjects	Parkinson patients
Mean Age + SD	65.71 ± 7.98	65.71 ± 8.05
Sex Ratio	21M/21F	22M/20F
Mean UPDRS	NA	25.23 ± 15.30
Mean LED	NA	361 ± 315.78
Mean H&Y	NA	1.54 ± 0.61
Mean duration of the disease	NA	6.10 years ± 4.27
Most affected side	NA	24 right / 18 left
Legend: UPDRS: Unified Parkinson Disease Rating Scale, LED: Levodopa Dose Equivalent, H&Y: Hoehn and Yahr Scale		

All participants had a structural MRI using a 3T head-only MRI-scanner (Magnetom Allegra, Siemens Medical Solutions, Erlangen, Germany) operated with an 8-channel head coil. Structural and quantitative maps of R_1, R_2*, effective proton density (PD*) and magnetization transfer saturation (MT) at 1 x 1 x 1 mm^3 resolution were calculated from a multi-parameter protocol based on a 3D multi-echo fast low angle shot (FLASH) sequence.

The VBQ toolbox implemented in SPM12(Callaghan et al., 2014; Helms et al., 2009; Weiskopf et al., 2013) was used for voxel-based analyses within the brain of the the MT, PD*, R1, R2* and grey matter maps,

All MRI data were segmented using unified segmentation(Ashburner and Friston, 2005) after creation of the parametric maps from the raw data, then spatially normalized to a population-specific template using diffeomorphic registration(Ashburner, 2007) (DARTEL) and smoothed using a 6mm FWHM kernel. Analyses were restricted to regions known to be affected in Parkinson s' disease basal ganglia and substantia nigra using an independent mask (available from https://www.nitric.org/projects/atag). We only report here results VBQ analysis for PD* and R2* maps, beside voxel based morphometry (VBM) analysis(Ashburner and Friston, 2000) for the grey matter maps. Group comparisons were performed voxel-by-voxel using SPM12 software. Statistical threshold was set at $p<0.05$, corrected for multiple comparisons using TFCE toolbox(Smith and Nichols, 2009) with 5000 permutations.

RESULTS

PD* maps

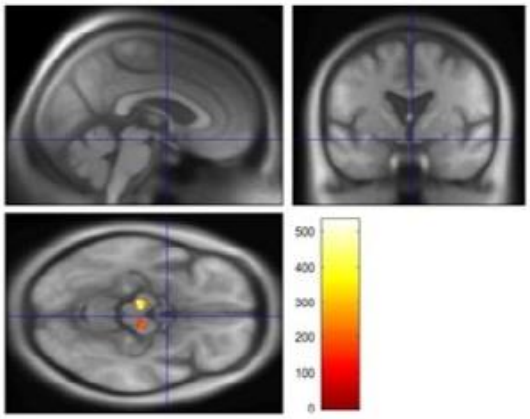

Figure A

R2* Maps

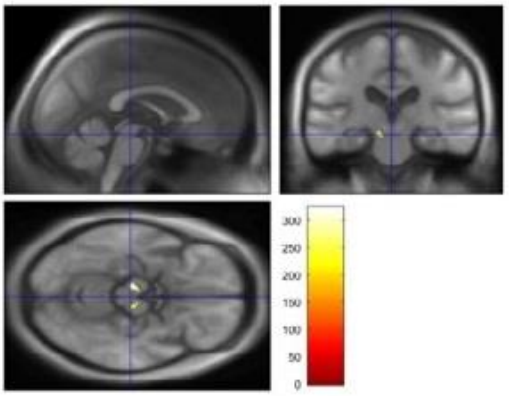

Figure B

Grey matter maps (VBM analysis)

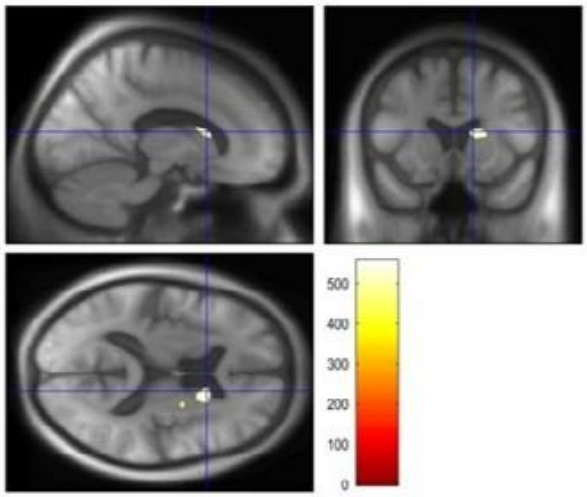

Figure C

Using PD* maps, we found a significant decrease in PD patients as compared to controls in the left and right substantia nigra (figure A, left panel). On the other hand, R2* was significantly increased in PD patients as compared to controls into symmetrical clusters located in the Substantia Nigra (figure B, right panel).

VBM analysis (figure C) showed the local grey matter volume was significantly decreased in PD patients, as compare to normal controls in the body of the right caudate nucleus.

CONCLUSION

Advanced quantitative MRI sequences such as MPM are able to show group differences in brain microstructure in brain regions known to be affected by neuropathological changes in

Parkinson's disease. We are currently conducting a validation study in a separate cohort and on a different scanner.

SUMMARY FOR LAY PEOPLE

Actuellement, le diagnostic de maladie de Parkinson (MP) s'appuie toujours sur des éléments essentiellement cliniques et les erreurs restent fréquentes, notamment avec des maladies voisines. Nous ne disposons pas encore d'un biomarqueur permettant un diagnostic de certitude et l'imagerie cérébrale de routine est réputée normale. Notre équipe a étudié la capacité de l'IRM cérébrale à détecter des anomalies spécifiques de la maladie par l'emploi de séquences quantitatives (« multi-parameter mapping »). En comparant un groupe de patients à un groupe contrôle, les analyses démontrent des anomalies de la microstructure cérébrale dans des régions connues pour être affectées par la MP.

ACKNOLEDGEMENTS

We would like to thank the MoVeRe Team, Pr. P. Maquet, E. Balteau and C. Phillips for their kind advice on this manuscript.

REFERENCES

Antoniades, C. A., and Barker, R. A. (2008). The search for biomarkers in Parkinson's disease: a critical review. *Expert Rev. Neurother.* 8, 1841–1852. doi:10.1586/14737175.8.12.1841.

Ashburner, J. (2007). A fast diffeomorphic image registration algorithm. *Neuroimage* 38, 95–113. doi:10.1016/j.neuroimage.2007.07.007.

Ashburner, J., and Friston, K. J. (2000). Voxel-based morphometry--the methods. *Neuroimage* 11, 805–21. doi:10.1006/nimg.2000.0582.

Ashburner, J., and Friston, K. J. (2005). Unified segmentation. *Neuroimage* 26, 839–51. doi:10.1016/j.neuroimage.2005.02.018.

Baudrexel, S., Nürnberger, L., Rüb, U., Seifried, C., Klein, J. C., Deller, T., et al. (2010). Quantitative mapping of T1 and T2* discloses nigral and brainstem pathology in early Parkinson's disease. *Neuroimage* 51, 512–20. doi:10.1016/j.neuroimage.2010.03.005.

Callaghan, M. F., Freund, P., Draganski, B., Anderson, E., Cappelletti, M., Chowdhury, R., et al. (2014). Widespread age-related differences in the human brain microstructure revealed by quantitative magnetic resonance imaging. *Neurobiol. Aging* 35, 1862–1872. doi:10.1016/j.neurobiolaging.2014.02.008.

Helms, G., Draganski, B., Frackowiak, R., Ashburner, J., and Weiskopf, N. (2009). Improved segmentation of deep brain grey matter structures using magnetization transfer (MT) parameter maps. *Neuroimage* 47, 194–8. doi:10.1016/j.neuroimage.2009.03.053.

Michaeli, S., Oz, G., Sorce, D. J., Garwood, M., Ugurbil, K., Majestic, S., et al. (2007). Assessment of brain iron and neuronal integrity in patients with Parkinson's disease using novel MRI contrasts. *Mov. Disord.* 22, 334–40. doi:10.1002/mds.21227.

Pyatigorskaya, N., Gallea, C., Garcia-Lorenzo, D., Vidailhet, M., and Lehericy, S. (2014). A review of the use of magnetic resonance imaging in Parkinson's disease. *Ther. Adv. Neurol. Disord.* 7, 206–220. doi:10.1177/1756285613511507.

Smith, S. M., and Nichols, T. E. (2009). Threshold-free cluster enhancement: addressing problems of smoothing, threshold dependence and localisation in cluster inference. *Neuroimage* 44, 83–98. doi:10.1016/j.neuroimage.2008.03.061.

Weiskopf, N., Suckling, J., Williams, G., Correia M., M. M., Inkster, B., Tait, R., et al. (2013). Quantitative multi-parameter mapping of R1, PD*, MT, and R2* at 3T: A multi-center validation. *Front. Neurosci.*, 1–11. doi:10.3389/fnins.2013.00095.